

# Design and Manufacturing of a Miniaturized 2.45GHz Bulk Acoustic Filter by High Aspect Ratio Etching Process

C.-H. Lin<sup>\*</sup>, H.-R. Chen<sup>\*\*</sup>, C.-H. Du<sup>\*\*</sup> and W. Fang<sup>\*</sup>

<sup>\*</sup>National TsingHua University, Hsinchu, Taiwan, [fang@pme.nthu.edu.tw](mailto:fang@pme.nthu.edu.tw)

<sup>\*\*</sup>Asia Pacific Microsystems, Inc., Hsinchu, Taiwan, [chdu@apmsinc.com](mailto:chdu@apmsinc.com)

## ABSTRACT

A 2.45GHz filter is fabricated by thin film bulk acoustic wave resonator (FBAR) technology. Especially, it is designed to minimize die size and to simplify fabrication process simultaneously by using inductive coupling plasma etching. The quality factor of fabricated single resonator is 1567 and electromechanical coupling coefficient is 5.7%. The fabricated filter has minimum insertion loss around 1.5dB and maximum insertion loss 3.6dB in 83.5MHz bandwidth, which is suitable for WLAN and Bluetooth applications.

**Keywords:** bulk acoustic device, ICP, MEMS resonator

## 1 INTRODUCTION

The requirements of filters become more and more significant as wireless communication systems develop into higher frequency region. FBAR is a promising technology for these high frequency filters, because it has high power handling capability and it can precisely controls the resonance frequency by thin film thickness. Presently, the fabrication method for FBARs can be classified into three categories: back-side wet etching processes [1,2], front-side etching process [3,4], and multi-layer reflection method [5,6]. However, the multi-layer reflection method requires carefully controlled thickness for each layer. The front-side etching process face obstacles at the releasing step when chemicals have low selectivity between surface devices and sacrificial layer. And the back-side wet etching process has drawbacks of large device size and also has difficulties in front-side protection. In this study, Inductive Coupling Plasma (ICP) back-side etching process was used. Since ICP provided high aspect ratio etching, small device size can be fabricated. Moreover, the dry etching and high material etching selectivity characteristics of ICP process solved the front-side protection problem.

## 2 DESIGN AND SIMULATION

Thin film bulk acoustic resonators operate like quartz resonators, except that they are fabricated by thin film technology, therefore the operation frequency is much higher than quartz resonators. A basic FBAR structure includes a piezoelectric layer between two electrode layers.

And the stacked structure is suspended so that both the top and bottom surface are free to deform in out-of surface direction. Since longitudinal acoustic wave perfectly reflect at free surfaces, e.g. solid-air interface, standing waves can be created in the FBAR structure. Piezoelectric film then transfers energy from acoustic standing waves to electrical resonance.

An accurate model is required to simulate the complex behavior of FBAR. In this work, acoustic transmission line model was used. This model treats every acoustic layer segments as microwave transmission lines using force-voltage analogy. In addition, conventional Mason equivalent circuit model was used for piezoelectric material, which comprised two acoustic ports and one electrical port [7]. Connecting Mason's piezoelectric model and acoustic transmission line models in series, frequency response of the stacked structure was simulated. Figure 1 demonstrated the simulated frequency response of the proposed FBAR. The relationship between resonance frequency and structure thickness was analyzed after many times of simulation. And a favorable thickness set, included bottom electrode layer, piezoelectric layer and top electrode layer was selected for the following fabrication processes.

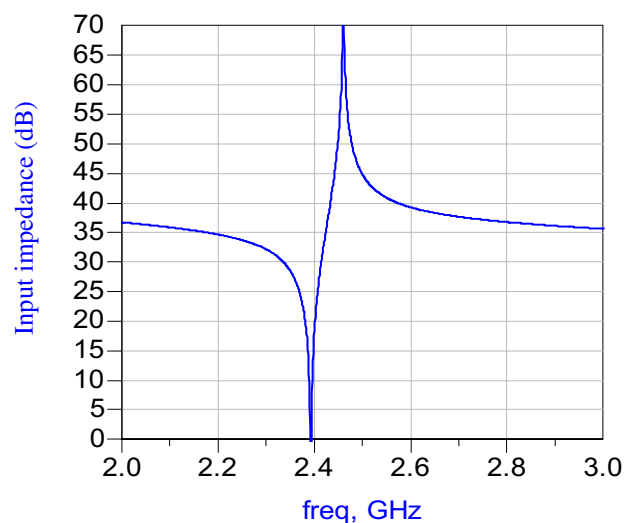


Figure 1: Simulation result of a bulk acoustic resonator using transmission line model.

### 3 PROCESS DESIGN AND RESULTS

Fabrication process is summarized in Figure 2. First, Silicon dioxide and nitride layers was grown and deposited as insulating layers and etching stop layers for ICP process (Fig. 2a). Next, bottom electrode was deposited and patterned (Fig. 2b). In this study, Ti-Pt was used, because Aluminum nitride (AlN) was selected to be the piezoelectric layer and AlN(002) structure can be better grown on properly oriented Pt. For the AlN deposition step, DC sputter process was used and the deposition temperature was below 400 °C (Fig. 2c). AlN was then etched by chemical solution to provide connection via between bottom electrode and top electrode. Then, the top electrode was deposited and the geometry was defined by lift-off process (Fig. 2d). The material of top electrode was Aluminum with low resistivity and low density. Additional thin metal layer was deposited on selective area to make thicker resonator devices, which had lower resonance frequencies. Afterward, backside ICP etching was used to remove silicon substrate and formed thin membranes (Fig. 2e). These membranes were free at top and bottom surfaces, therefore resonators can achieve high quality factor. Finally, insulating layers under membrane was removed to increase quality factor and fine tune resonance frequency (Fig. 2f).

The fabricated devices was designed to have compact size smaller than 1mm×1mm, therefore the total number of devices on the six-inch wafer was about 10,000. Figure 3 shows the cross section view of one suspended FBAR filter, the cavity size was less than 600 um×600 um×600um, and it had vertical walls perpendicular to wafer surface. This characteristic of ICP etching process largely reduced the device size as expected. Figure 4 shows the membrane structure. The micrometer-thick AlN film had grown well on the Ti-Pt film, and collimate structure throughout the layer can be observed.

### 4 MEASUREMENT RESULTS

To demonstrate the performance of this design, two types of acoustic devices were measured. First, a resonator test key was employed to identify the quality factor. Next, filters were measured and compared to required specifications. The devices were characterized by network analyzer and on-wafer probe.

Resonator test keys were tested by one-port test method. Moreover, in order to demonstrate the overall performance of the resonator device, the parasitic resistance was not de-embedded in measurement. Test results of resonators are shown in Figure 5 and 6. Figure 5 shows the resonator S11 in the form of smith chart. Very small effective series resistance presented and shrunk the measured S11 circle. However, this small amount of series resistance was acceptable for further filter design.

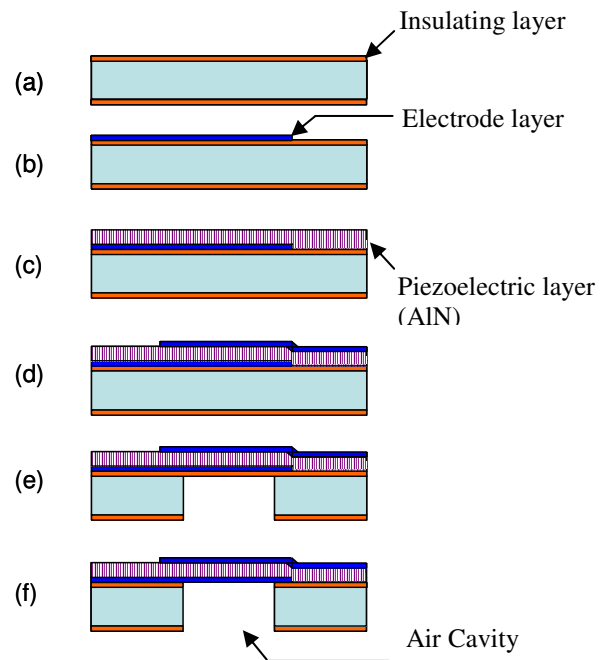


Figure 2: FBAR fabrication process using backside ICP.

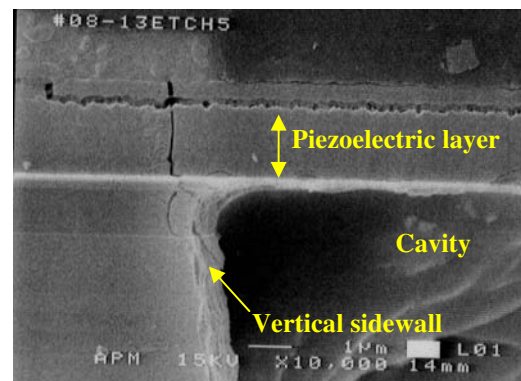


Figure 3: Cross section view of the fabricated device.

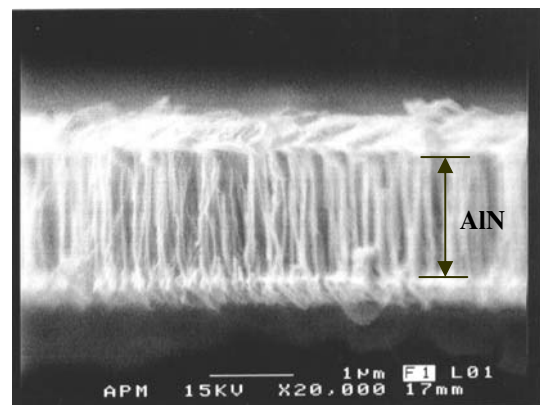


Figure 4: Collimated structure of AlN can be identified in the suspended membrane.

Figure 6(a) shows the magnitude of input impedance. One resonance point and one anti-resonance point could be determined by the minimum and maximum input impedance respectively. A good resonator for filter application should have wide separation between these two points, which represents the electromechanical coupling coefficient ( $K^2$ ). Higher  $K^2$  facilitates a wide band filter design and fabrication. From the resonance frequency ( $f_r$ ) and anti-resonance frequency ( $f_a$ ), the  $K^2$  was calculated by:

$$K^2 = \frac{\frac{\pi f_r}{2 f_a}}{\tan\left(\frac{\pi f_r}{2 f_a}\right)} \quad (1)$$

The measured  $K^2$  of this device was about 5.7%.

Figure 6(b) shows the phase of input impedance. For an ideal resonator, the phase should change from -90 to +90 degree in near vertical slope at resonance point. However, if some loss occurred in the resonance, the phase change became gentle. For this device, the phase change was quite steep, therefore the resonance had very high performance. The quality factor ( $Q$ ) was calculated by the rate of phase change with frequency:

$$Q_r = \frac{f_r}{2} \left| \frac{d\angle Z_{in}}{df} \right| \quad (2)$$

The quality factor was calculated to be 1567 for this device. The electrical performances had shown that the ICP process was promising for the fabrication of bulk acoustic resonators.

Temperature characteristic was also tested with thermal chuck and wafer probing method. The temperature was controlled to rise from 25 °C to 80 °C and then cool down from 80 °C to 5 °C. Resonance frequencies were recorded and plot in Figure 7. The measured relationship between temperature and resonance frequency was linear and had temperature coefficient of resonance frequency about -27.4 ppm/°C, which was consistent with studies done by other research groups. After the device temperature cooled from high temperature to room temperature, the resonance frequency returned to its original value at room temperature. This results indicated that although bulk acoustic wave devices using ICP method was suspend as a membrane, it still hold good thermal conductivity, and no heat pile up in the device during temperature raise and fall period.

Next, the filter performance was measured. This filter was a traditional ladder type design, it included three serially connected resonators and four shunt resonators. Figure 8 shows the typical measurement result. The

minimum insertion loss was about 1.5 dB, maximum insertion loss in 83.5MHz bandwidth was 3.6 dB, and minimum rejection was 25dB. According to the test results, this high frequency filter had good electric performance and meets the required specification. Other frequency bands range from 1.5GHz to 2.2GHz also could be redesigned and fabricated by changing the electrode layout and thickness of suspended membrane.

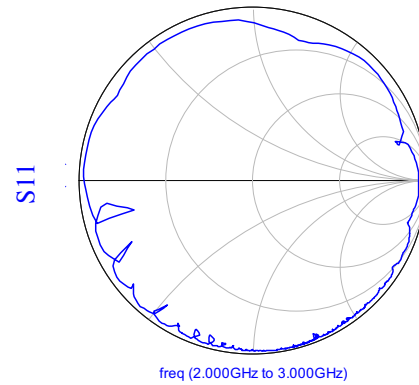


Figure 5: Measured resonator characteristic in smith chart form.

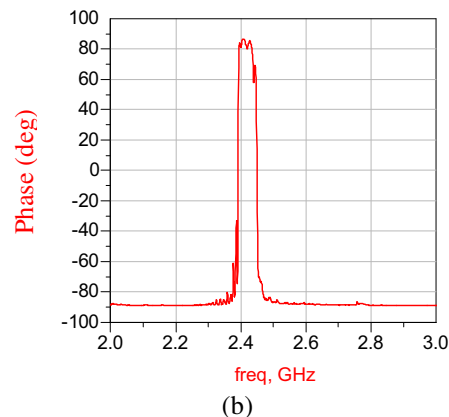
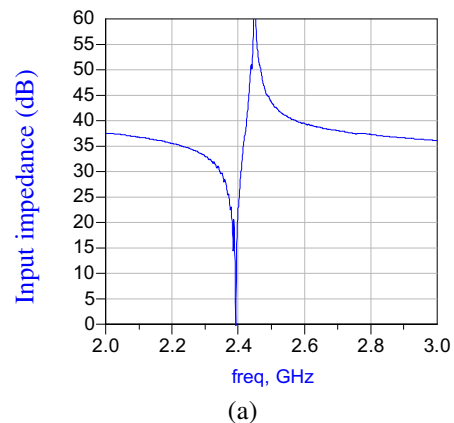


Figure 6: Measured input impedance, (a) magnitude, (b) phase.

## 5 CONCLUSION

Thin film bulk acoustic resonators and filters were fabricated using ICP process to reduce device size and facilitate fabrication process. Transmission line model was used to simulate the final resonator performance. And a preferable structure thickness was designed according to the simulation. Fabrication results demonstrated a small size device with near vertical cavity walls. The devices were tested by network analyzer and probe station. Quality factor and electromechanical coupling coefficient of a single resonator were 1567 and 5.7% respectively. Designed filter had maximum 3.6 dB insertion loss in 83.5 MHz band, rejection was more than 25dB. These fabrication results and test results confirmed that high quality thin film bulk acoustic resonators and filters can be designed and fabricated using ICP process.

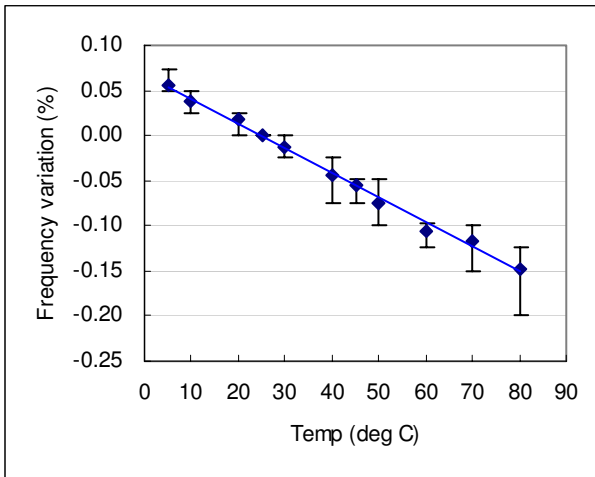


Figure 7: Relationship between temperature and variation of resonance frequency.

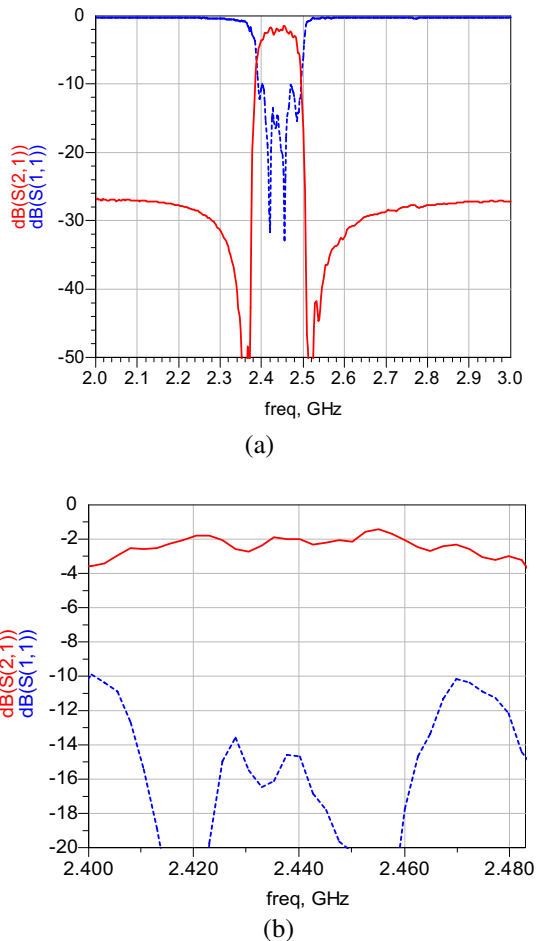


Figure 8: Filter performance (a) wide band, (b) narrow band.

## REFERENCES

- [1] Krishnaswamy, S.V., Rosenbaum, J., Horwitz, S., Vale, C. and Moore, R.A. "Film bulk acoustic wave resonator technology," Proceedings, IEEE Ultrasonics symposium, Honolulu, HI, December, 1990, pp 529-536.
- [2] Park, J.Y., Lee, H.C., Lee, K.H., Lee, H.M. and Ko, Y.J. "Micromachined FBAR RF filters for advanced handset applications," IEEE International conference on solid state sensors, actuators and microsystems, Boston, MA, June, 2003, pp 911-914.
- [3] Ruby, R., Bradley, P., Larson III, J.D. and Oshmyansky, Y., "PCS 1900MHz duplexer using thin film bulk acoustic resonator (FBARS) ," Electronics Letters, 35, pp 794-795, 1999.
- [4] Larson III, J. D., Ruby, R. C., Bradley, P. D., Wen, J., Kok, S-L, and Chien, A., 2000, "Power handling and temperature coefficient studies in FBAR duplexers for the 1900 MHz PCS band," 2000 IEEE Ultrasonics Symposium, San Juan, Puerto Rico, Vol. 1, pp. 869-874.
- [5] Lakin, K.M., McCarron, K.T. and Rose, R.E. "Solidly mounted resonators and filters," Proceedings, IEEE Ultrasonics Symposium, Seattle, WA, November, 1995, pp 905-908.
- [6] Yoon, G. and Park, J.D. "Fabrication of ZnO-based film bulk acoustic resonator devices using W/SiO<sub>2</sub> multilayer reflector," Electronics Letters, 36, pp 1435-1437, 2000.
- [7] Auld, B. A., 1973, Acoustic fields and waves in solids, John Wiley and Sons, New York.